2010

The Fundamental Gap For Hyperbolic Triangles

Dennis Stuart Fillebrown
Bucknell University

The Fundamental Gap for Hyperbolic Triangles

Dennis S. Fillebrown

A Thesis Submitted to the Honors Council

for Honors in Mathematics

May 3rd, 2010

Approved by:

Emily B. Dryden

Advisor: Dr. Emily Dryden

Karl Voss

Department Chair: Dr. Karl Voss

Contents

List of Tables

List of Figures

Abstract

In 1983, M. van den Berg made his Fundamental Gap Conjecture about the difference between the first two Dirichlet eigenvalues (the fundamental gap) of any convex domain in the Euclidean plane. Recently, progress has been made in the case where the domains are polygons and, in particular, triangles. We examine the conjecture for triangles in hyperbolic geometry, though we seek an for an upper bound for the fundamental gap rather than a lower bound. The Dirichlet eigenvalues of most polygons, including arbitrary hyperbolic triangles, cannot be calculated explicitly. However, the eigenvalues of disks are generally known. We take advantage of this fact by calculating the eigenvalues of the disks whose boundaries are the inscribed and circumscribed circles for a given triangle. We can relate the eigenvalues of these two disks to the eigenvalues of the triangle through domain monotonicity. Then, using a relationship between the eigenvalues of Euclidean and hyperbolic disks, an upper bound for the first eigenvalue of a Euclidean disk, and a lower bound for the first eigenvalue of a hyperbolic disk, we find an upper bound for the fundamental gap for hyperbolic triangles. We search for a nicer expression for the upper bound by examining the calculated upper bound numerically, leading to the following conjecture.

Conjecture: Let T be any hyperbolic triangle with angles between 0 and $\frac{\pi}{2}$ radians, an inscribed circle of radius r_I, and suppose that there exists a circumscribed circle of T. If λ_i^T denotes the Dirichlet eigenvalues of T, then

$$\lambda_2^T - \lambda_1^T \leq 10.2 \left(\frac{\pi}{r_I}\right)^2 . \tag{0.1}$$

1 Introduction

Every bounded region in the plane can easily be thought of as a drum head that can vibrate up and down. The boundaries of these so-called drum heads are fixed; that is, only the interior of the drum heads can move up and down. As a result, every such region has a set of frequencies at which it vibrates naturally based on the shape of the surface. This concept has been studied extensively in two directions: finding the frequencies at which a specific drum head can vibrate and the inverse problem of determining the shape of the drum based on knowledge of the frequencies. Both problems have been considered for some time. Attention was brought to the latter problem in 1966 by Mark Kac [12], who asked the simple question "Can one hear the shape of a drum?" The answer was shown to be no by Carolyn Gordon, David Webb, and Scott Wolpert in 1992 [9], [10]. They showed that two differently shaped drums could vibrate at the same set of natural frequencies and so would be indistinguishable simply by sound. However, we will be more interested in the former problem: given a drum head, can we determine the frequencies at which it can vibrate? While determining every such frequency would be ideal, it is likely an unrealistic goal. Regardless of other qualities of the frequencies, we must be able to order them from lowest to highest. As such, it is natural to investigate them in order from lowest to highest. In particular, we are interested in the difference between the first two frequencies at which triangular drum heads can vibrate. This area has been studied before and we begin with a presentation of the previous work and further motivation.

2 The Fundamental Gap

In order to investigate the frequencies at which triangular drums can vibrate, we need to set some initial mathematical framework. We first define the drum heads and the vibrational frequencies in explicit mathematical terms. We then give the recent progress that has been made towards finding these frequencies and why the difference between the first two frequencies is of interest. Finally, we summarize our main goals and outline the methods used herein.

2.1 The Conjecture

In 1983, M. van den Berg made a conjecture about the difference between the first two natural frequencies at which a drum can vibrate [20]. This conjecture, now called the Fundamental Gap Conjecture, motivates the remainder of our discussion and so we must define it in precise terms, which requires several definitions. First, we must explicitly define what we are considering as a drum head. This refers to any convex domain in the standard Euclidean plane. A *convex domain* is a region of the plane that has the property that for any two points inside the domain, the line connecting the two points is also contained within the domain. Figure 1 shows two convex domains and one non-convex domain. Every convex domain has a *diameter* which is the greatest distance between any two points on the boundary of the domain, e.g. a diagonal of a square. The diameter is a general measurement of the size of the domain.

Next, we must also define the natural frequencies mentioned. They are the eigenvalues of an operator acting on smooth functions on the domain. For brevity, we simply refer to these as the eigenvalues of the domain throughout the our discussion. More specifically, the frequencies are the Dirichlet eigenvalues of the domain. The Dirichlet eigenvalues of a convex domain Ω are the values

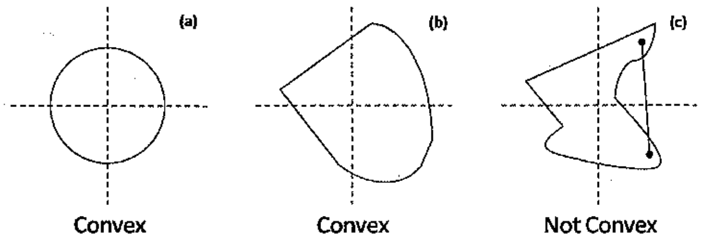

Figure 1: The domains shown in (a) and (b) are convex, while the domain in (c) does not satisfy the condition to be convex.

of λ for which the following is satisfied for some unknown function $u(x, y)$:

$$\begin{aligned} \Delta u + \lambda u &= 0 \text{ in } \Omega, \\ u|_{\partial\Omega} &= 0, \end{aligned} \tag{2.1}$$

where Δ is the Laplace operator defined as

$$\Delta u = \frac{\partial^2 u}{\partial x^2} + \frac{\partial^2 u}{\partial y^2}, \tag{2.2}$$

and $u|_{\partial\Omega}$ is the function u restricted to the boundary of Ω. There are infinitely many solutions $\lambda_1, \lambda_2, ...$ to (2.1) and by convention we order them in ascending order, so that $0 < \lambda_1 \leq \lambda_2 \leq .... \to \infty$. Then the fundamental gap for Ω is defined to be $\lambda_2 - \lambda_1$. With these two definitions, we can now state the Fundamental Gap Conjecture.

Fundamental Gap Conjecture (M. van den Berg): Let Ω be any convex domain with diameter d and Dirichlet eigenvalues $0 < \lambda_1 \leq \lambda_2 \leq \lambda_3 \leq ....$. Then

$$d^2 (\lambda_2 - \lambda_1) \geq 3\pi^2. \tag{2.3}$$

Notice that given any convex domain Ω, this conjecture does not tell us what the first two Dirichlet eigenvalues are and it certainly does not give us the entire list. However, having information about the fundamental gap of a convex domain is useful and this conjecture gives a relatively simple lower bound. In particular, its greatest strength lies in the fact that knowing the diameter of Ω is enough to find the lower bound. So we have a lower bound for the fundamental gap determined entirely by a single geometric quantity (the diameter) associated with a given convex domain.

The other key aspect to note about the Fundamental Gap Conjecture is that it is a conjecture about every convex domain. In general, two arbitrary convex domains have little to nothing in common. Thus proving this conjecture for every convex domain simultaneously is likely a difficult goal, an assertion supported by the lack of progress towards a proof in the 27 years since the conjecture was stated by van den Berg. An alternative approach is to choose a specific set of convex domains that share some basic properties and work towards proving the Fundamental Gap Conjecture about that set of domains. This is the direction which was taken recently when progress was made towards proving the conjecture for polygonal domains and, in particular, triangular domains.

2.2 Recent Progress

Recent work by Lu and Rowlett [15] focused on proving the Fundamental Gap Conjecture for polygonal domains. The fundamental gap for Euclidean domains and, most importantly, polygonal domains is especially interesting because of its physical significance in many areas. Of particular importance is shape recognition of either surfaces or solids [17]. The eigenvalues can be used as a "Shape-DNA", a type of mathematical signature, to help identify any surface or solid. Having such a signature helps for many tasks, including database retrieval, shape matching, and even quality assessment. Though knowing the exact eigenvalues would be ideal, they cannot be found explicitly in general and so information on the fundamental gap can help fill in the missing information.

Focusing mostly on triangles, Lu and Rowlett produced numerical evidence supporting the Fundamental Gap Conjecture for all triangles in the Euclidean plane. They were also able to prove that the fundamental gap is unbounded for collapsing triangles that have two angles α and β satisfying $\frac{2}{3} \leq \frac{\alpha}{\beta} \leq 1$. We will outline their basic procedure. As mentioned above, calculating the Dirichlet eigenvalues of a given domain can only be done explicitly in a handful of cases. Instead, Lu and Rowlett bounded a given triangle by two circular sectors, which are pieces of a disk (see Fig. 2) [15]. The Dirichlet eigenvalues of disks, and therefore circular sectors, can be explicitly calculated. The eigenvalues of sectors are related to the eigenvalues of the triangle through a property known as *domain monotonicity*. Indeed, let Ω and Ω' be two convex domains with Dirichlet eigenvalues $\lambda_1, \lambda_2, \cdots$ and $\lambda'_1, \lambda'_2, \cdots$ respectively. Then domain monotonicity is the property that if $\Omega \subset \Omega'$, then $\lambda_l \geq \lambda'_l$ for all l. In other words, if one convex domain Ω is contained in another Ω', then the eigenvalues of Ω are larger than the corresponding eigenvalues of Ω'. The results obtained by Lu and Rowlett are also the start of a general program for proving the conjecture for all polygons.

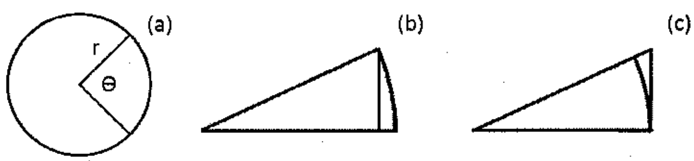

Figure 2: The region between the two radii in (a) is a sector of angle θ. For any triangle, we can find the minimal sector containing the triangle (b), and the maximal sector contained in the triangle (c). Calculating the Dirichlet eigenvalues of these two sectors gives us a good estimate of the Dirichlet eigenvalues of the triangle.

2.3 Main Goal

The Fundamental Gap Conjecture posits an explicit lower bound for the fundamental gap for any convex domain in the Euclidean plane. The conjecture does not give any indication as to whether or not there is an upper bound for the fundamental gap or what that bound might be if it exists. We mentioned that Lu and Rowlett do examine this issue and discover that the fundamental gap is unbounded for a certain class of triangles [15]. In 1985, Singer *et al.* found an upper bound for the fundamental gap of a slightly different operator [21, p. 230]. The upper bound was given for the fundamental gap for the Schrödinger operator, which is closely related to the problem given in Eq. (2.1). The eigenvalues of the Schrödinger operator on a convex domain Ω in $\mathbb{R}^2$ are the values λ for which

$$\begin{aligned} -\Delta u + Vu &= \lambda u, \\ u &= 0 \text{ on } \partial\Omega, \end{aligned} \tag{2.4}$$

is satisfied where V is a non-negative function defined on the closure of Ω, denoted $\bar{\Omega}$, and $u(x, y)$ is again an unknown function. In [21], it is shown that

$$\lambda_2 - \lambda_1 \leq \left(\frac{8\pi^2}{D^2} + \frac{4(M-m)}{2}\right), \tag{2.5}$$

where D is the diameter of the largest inscribed ball in Ω and $M = \sup_{\bar{\Omega}}(V)$ and $m = \inf_{\bar{\Omega}}(V)$. However, if we let V be the zero function, we see that Eq. (2.4) reduces to Eq. (2.1) and $M = m = 0$. Then an upper bound for the fundamental gap for convex domains in $\mathbb{R}^2$ is given by

$$\lambda_2 - \lambda_1 \leq 8\left(\frac{\pi}{D}\right)^2. \tag{2.6}$$

Similar to the Fundamental Gap Conjecture, this upper bound for the fundamental gap is only dependent on the size of the domain and, in particular, the size of the largest ball inside that domain. Instead of further examining this upper bound, we look to take the idea of finding an upper bound for the fundamental gap of a convex domain in a slightly different direction. We consider the Dirichlet eigenvalues of convex domains in hyperbolic geometry and in particular, the fundamental gap for hyperbolic triangles.

Our approach will be similar in nature to that of Lu and Rowlett. As mentioned above, Lu and Rowlett bounded a triangle with two sectors and used domain monotonicity to relate the eigenvalues of the sectors to the eigenvalues of the triangle. We will use the same technique, but replace sectors with an inscribed and a circumscribed circle. Then the domain monotonicity will once again reveal properties of the eigenvalues of the triangles. The main advantage to circles over sectors here is that while the eigenvalues of sectors are not very well understood in hyperbolic geometry, there is a reasonable amount of knowledge about the eigenvalues of disks. Using these techniques, we find an upper bound for the fundamental gap for triangles in hyperbolic geometry, similar to Eq. (2.6). To begin, we must first understand hyperbolic geometry and how it differs from the familiar Euclidean setting.

3 Hyperbolic Space

The geometry with which we are all familiar is known as Euclidean geometry. It is the geometry that generally arises in the world around us and so is the most practical to study. However, it is not the only geometry in which one can work. There are two other geometries that at first appear to have nothing in common with Euclidean geometry, but upon further inspection, are actually quite similar. We begin by exploring the foundations of Euclidean geometry and then examine how to alter the familiar setting to produce one of the other two geometries, hyperbolic geometry.

3.1 Axiomatic Geometry

The general rules of Euclidean geometry are natural to almost every student: lines intersect at only one point, every triangle has angle sum π radians etc. While these ideas may seem to be the basis for Euclidean geometry, we can dig a little deeper to uncover a more basic set of rules. Euclidean geometry can actually be built from a set of axioms that determine every other property that we know about our familiar geometry [11, pp. 597-598]. We take many of these axioms for granted, such as the axiom that if there are three distinct points lying on the same line then only one point is between the other two [11, p. 105]. The most important axiom of Euclidean geometry is known as the parallel postulate. It states that for any line l and any given point P not on l, there is exactly one line through P parallel to l (see Figure 3).

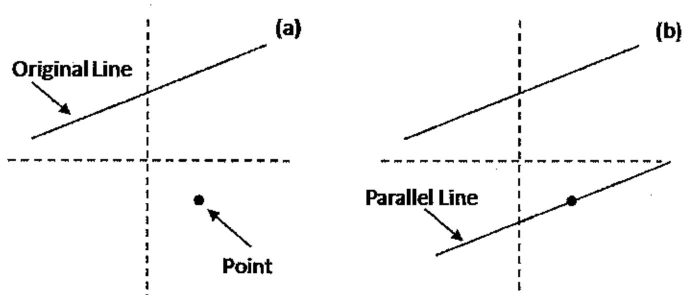

Figure 3: In familiar Euclidean geometry, the second line in (b) is the only line parallel to the original line through the given point. This is not the case in other geometries.

Though this axiom seems natural to those who have become accustomed to Euclidean geometry, it is actually the axiom upon which all of Euclidean geometry rests. Without this axiom, for instance, we can use the remaining axioms to construct a four-sided figure with 3 right angles and one non-right angle, which is an absurd notion in Euclidean geometry. It is the parallel postulate that guarantees that the fourth angle must also be a right angle. However, there is no mathematical reason why we must accept the parallel postulate: we can build many consistent geometries from the remaining axioms. A geometry obtained from doing so is known as a neutral geometry. Furthermore, there are two natural alternatives to the parallel postulate that we may add to a neutral geometry that give us two entirely different geometric settings. We consider one of those alternatives here. We replace the parallel postulate with the following: for any line l and a given point P not on l, there are at least two lines parallel to l through P [11, p. 250]. It turns out that this condition implies that for any l and P, there are infinitely many lines parallel to l through P. Adding this assumption to the axioms of neutral geometry gives us hyperbolic geometry. This is initially very unintuitive to imagine. However, there is a simple model of hyperbolic geometry which demonstrates the unfamiliar condition on parallel lines. In order to explain the model, we require some preliminary definitions.

3.2 Metrics, Geodesics, and Curvature

Before we can consider our new geometric setting, we need to develop a more precise language for describing distances and lines in a general geometry. Given a set, a *metric* on that set is a function that describes distances between the elements of that set [2, p. 328]. In particular, a *metric* on a set X is a function $d : X \times X \to \mathbb{R}$ that satisfies the following properties for all x, y, $z \in X$:

1. $d(x, y) \geq 0$,

2. $d(x, y) = 0 \quad \text{if and only if} \quad x = y$,

3. $d(x, y) = d(y, x)$,

4. $d(x,z) \leq d(x,y) + d(y,z)$.

For example, we can consider the familiar (x, y) coordinate plane as a set. Usually, we describe the distance between two points (x_0, y_0) and (x_1, y_1) by the distance formula, $d = \sqrt{(x_1 - x_0)^2 + (y_1 - y_0)^2}$. This distance function is a metric on the plane and one can show that it satisfies the properties listed above. Though it is the natural metric, it is not the only one. We could define the distance between two pairs of points as $d_1 = |x_1 - x_0| + |y_1 - y_0|$. This is known as the taxi-cab metric, since to get between two points, one is only permitted to travel horizontally or vertically, the way a taxi-cab must navigate through city streets. Again, we can check that this does indeed define a metric on the (x, y) plane. In general, every set can be given many metrics and the particular application determines which is used.

Once a set has been given a metric and we have a way to measure distances, a natural next step is to try and find the shortest distance between elements of the set. This shortest distance is realized by a curve called a *geodesic*. In familiar Euclidean geometry, the shortest distance between any two points is realized by a straight line: thus the geodesics of Euclidean geometry are straight lines. Now consider a slightly different setting, a sphere. The shortest distance between two points is now realized by the portion of the great circle on the surface of the sphere that passes through both points. Thus the geodesics on the sphere are all of the great circles. The same set with different metrics will also have different geodesics.

The final concept that we require is that of *curvature* of a surface, denoted κ. Unfortunately, the technical definition is beyond the scope of our work here and so we give just a basic idea of the concept. As its name might suggest, curvature is a way of measuring how much a given surface curves. Areas where the surface is mostly flat have small curvature and areas that have sharp bends have large curvature. The curvature of a surface can vary from point to point and can be drastically different throughout a surface. If a surface has the same curvature at all points, then it is known as a surface of constant curvature. The Euclidean plane is an example of such a surface and has curvature 0 everywhere. The model of hyperbolic geometry presented in the next section also has constant curvature of $\kappa = -1$ [11, pp. 484-487]. Curvature is not necessary for a description of the model, but will be required later. With these generalized notions of distance and straight lines, we can proceed to define our model of hyperbolic geometry.

3.3 Model of Hyperbolic Geometry

With the concepts of geodesics and metrics, we can describe a simple model of hyperbolic geometry [11, pp. 74]. Let S^1 denote the unit circle. We will discuss later the metric for this model; for now let the geodesics be either a diameter of the circle or a portion of a circular arc that intersects S^1 orthogonally (at right angles) and define "points" to be regular Euclidean points within the disk bounded by S^1. This is a model of hyperbolic geometry and satisfies all of the axioms of neutral geometry plus the new parallel axiom. Indeed, take any small portion of an orthogonal arc contained in the disk bounded by S^1. Then taking P as the center of the disk, we can find as many diameters through P as we wish that do not intersect the portion of the arc, as seen in Figure 4. This is the model of hyperbolic geometry, known as the Poincaré Disk, that we will be referencing throughout.

4 Polar Coordinates

The other decision that we must make is what coordinate system we will use. In general, standard Cartesian coordinates (x, y) are good for describing figures and regions consisting of mostly straight lines. We are more interested in describing

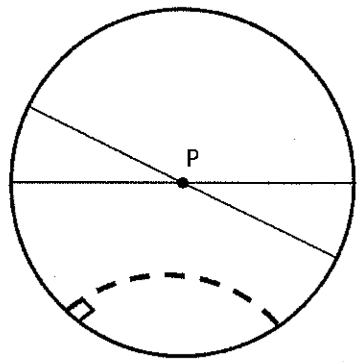

Figure 4: In hyperbolic geometry, there are infinitely many lines through a given point parallel to a given line. The two lines through the center of the disk are both parallel to the dotted line and all three are geodesics in the Poincaré Disk model. It is easy to see how we could find as many geodesics as we wish passing through the center of the disk and parallel to the dotted line.

curved and circular regions. To do so, we will use polar coordinates. The next two sections describe polar coordinates in both Euclidean and hyperbolic geometry.

4.1 Euclidean Case

Usually, we describe a point in the Euclidean plane by (x, y) coordinates. This approach is the familiar one and works extremely well for dealing with straight lines and other rectangular objects. However, these coordinates become cumbersome when dealing with circular regions. Polar coordinates are designed to make dealing with circular objects simple. Instead of a point being given in coordinates (x, y), it is specified by (r, θ) [19, pp. 705-707]. The coordinate r is known as the radius and is the straight line distance from the origin $(0, 0)$ to the point of interest. For example, the point $(1, 1)$ is $\sqrt{2}$ units away from the origin by the distance formula, so $r = \sqrt{2}$. The other component, θ, is a measure of angle. To understand θ, consider an arrow emerging from the origin that rests on the right half of the x-axis. We can rotate this arrow counterclockwise around the origin, creating some angle between the arrow and the x-axis. We rotate this arrow until it is pointing in the direction of the point that we are interested in. In the case of $(1,1)$, we would have to rotate the arrow $\pi/4$ radians counterclockwise. Thus $\theta = \pi/4$. So transforming $(1,1)$ from Euclidean to polar coordinates gives us $(\sqrt{2}, \pi/4)$, as shown in Figure 5.

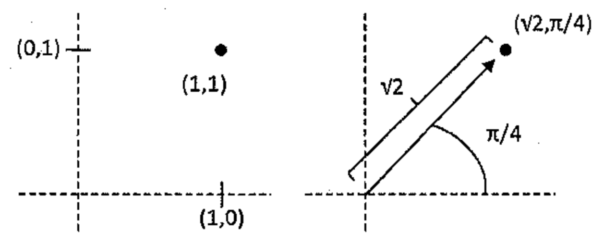

Figure 5: The point $(1,1)$ in (x,y) coordinates becomes the point $(\sqrt{2}, \pi/4)$ in polar coordinates.

The advantage of polar coordinates is that circular objects are very easily described. Indeed, a circle of radius r is simply all points (r,θ) for $0 \leq \theta \leq 2\pi$. Since we are interested in describing circles in the Poincaré Disk model, using a coordinate system that easily describes curves will make our computations easier [11].

4.2 Hyperbolic Case

Polar coordinates in hyperbolic geometry have a similar feel to their Euclidean counterpart in that they have a radial and angular component. Since we will be using the Poincaré Disk as our model of hyperbolic geometry, our definition is given in terms of this model [5, pp. 1-4]. Let p_0 be the center of the Poincaré Disk. For any point p in the disk, there is a unique geodesic η through p and p_0. Fix a vector v based at p_0 to play the role that the positive x-axis plays in Euclidean polar coordinates; v is known as the *polar axis*. Let σ be the angle from v to the tangent vector to η at p_0 and let ρ be the distance from

p_0 to p, as shown in Figure 6. The coordinates (ρ, σ) are known as the polar coordinates of p with respect to p_0 and v. Notice the similarity to Euclidean polar coordinates: both types have a radial coordinate to convey a distance and an angular coordinate to convey direction. These coordinates are more natural to use for the domains that we are considering.

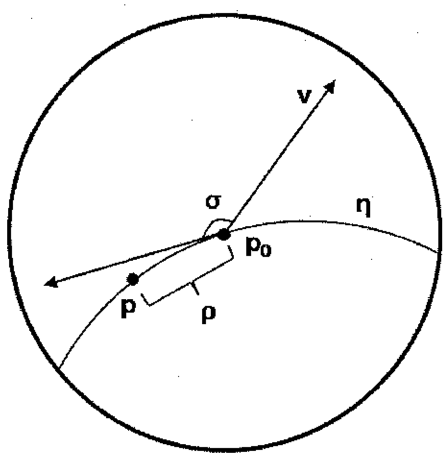

Figure 6: To describe a point in the Poincaré disk in polar coordinates, we let p_0 be the center of the disk. For a given point p, we take the unique geodesic η through p_0 and p. We pick any vector v, called the polar axis, emanating from p_0 and take a vector tangent to η at p_0. We then find the angle σ between v and the tangent to η at p_0. Lastly, we find the distance ρ along η between p and p_0. Then the hyperbolic polar coordinates of p with respect to p_0 and v are (ρ, σ).

5 Polar Laplacian

Changing our coordinate system means we must make some other changes as well. In particular, we can no longer use the expression for the Laplacian given in Eq. (2.2) since the terms $\frac{\partial^2 u}{\partial x^2}$ and $\frac{\partial^2 u}{\partial y^2}$ are given with respect to x and y and our coordinates are now given with respect to either r and θ or ρ and σ. As such, we need to convert the expression for the Laplacian to one that is dependent on r and θ or ρ and σ for the Euclidean and hyperbolic cases, respectively. The next two sections provide the details for these transformations.

5.1 Rectangular to Polar

Recall that the Laplacian is given in rectangular coordinates by (2.2) as

$$\Delta u = \frac{\partial^2 u}{\partial x^2} + \frac{\partial^2 u}{\partial y^2}. \tag{5.1}$$

In order to make the switch from Euclidean coordinates to polar coordinates, we require a relation between the two sets of coordinates. It is well known that the formulae

$$\begin{aligned} x &= r\cos(\theta), \\ y &= r\sin(\theta), \\ \theta &= \tan^{-1}\left(\frac{y}{x}\right), \\ x^2 + y^2 &= r^2, \end{aligned} \tag{5.2}$$

convert between a Cartesian coordinate (x, y) and a polar coordinate (r, θ) [19, pp. 706-707]. The details of the derivation of the Laplacian in polar coordinates are lengthy and so are given in Appendix A. In general, the process is straightforward and is simply a matter of substitution according to Eq. (5.2) and applying the Chain Rule. The result is that the Laplacian in polar form is given by

$$\Delta u = \left(\frac{\partial^2 u}{\partial x^2} + \frac{\partial^2 u}{\partial y^2}\right) = \frac{\partial^2 u}{\partial r^2} + \left(\frac{1}{r}\right)\frac{\partial u}{\partial r} + \left(\frac{1}{r^2}\right)\frac{\partial^2 u}{\partial \theta^2}. \tag{5.3}$$

Using this expression for the Laplacian, we can find the eigenvalues using the method of separation of variables. We outline the process here and provide the derivation in Appendix B. We begin by assuming that a function F can be separated into two functions, one dependent only on r and one dependent only on θ, so that $F(r,\theta) = R(r)\Theta(\theta)$. Then we take the equation $\Delta F + \lambda F = 0$ and apply the Laplacian to our function F. We can separate the variables so that we have an expression involving only r equal to an expression involving only θ. However, r and θ change independently, so a change in r does not imply a change in θ and vice versa. Thus both expressions must be constant and so we can set both expressions equal to that constant, denoted k^2, resulting in two differential equations, one involving $R(r)$ and one involving $\Theta(\theta)$. The equation involving $\Theta(\theta)$ turns out to be the expression for the Laplacian on a sphere and determines the values of k to be $0, 1, 2, 3, \cdots$. We can use these values for k when solving for $R(r)$. We find that solutions for $R(r)$ are Bessel functions, a well studied class of functions, and that the values of λ are the zeros of these functions. We will discuss Bessel functions in more detail in Section 7.1. However, we will mention now that enough is known about Bessel functions that their zeros can be calculated numerically which makes explicitly calculating the eigenvalues of Euclidean disks relatively easy. The eigenvalues of the Laplacian in the hyperbolic case also turn out to be the zeros of a known, though more complicated, class of functions as we see in the next section.

5.2 Poincaré Disk Laplacian

Now we move on to the case of hyperbolic geometry. Since we will be using the Poincaré Disk model of hyperbolic geometry, we wish to find an expression for the Laplacian in this model. We start from the rectangular metric tensor on the Poincaré Disk; a metric tensor is the analog of a metric on a Riemannian manifold. Informally, an n-dimensional Riemannian manifold is an n-dimensional object that "looks like" and behaves like $\mathbb{R}^n$ in small patches and a metric tensor is a way to measure distances on a Riemannian manifold. We do not require a precise definition for metric tensors since we are only working with the expression formally. The standard metric tensor on the Poincaré Disk is known to be [11, p. 565]

$$ds^2 = \frac{4(dx^2 + dy^2)}{(1 - (x^2 + y^2))^2}. \tag{5.4}$$

One will notice that the numerator of Eq. (5.4) contains the standard rectangular metric tensor in the Euclidean plane. The denominator accounts for the fact that shorter distances nearer the boundary of the Poincaré Disk are the same as longer distances closer to the center of the disk. Now we use the substitutions

$$x = \tanh(r/2)\cos(\sigma)$$
$$y = \tanh(r/2)\sin(\sigma)$$

given in [16, p. 210] to convert from rectangular to hyperbolic polar coordinates. Once again, this derivation is too lengthy to be given here and as such is given in Appendix C. However, the process is generally the same as for the Euclidean case, in that it requires substitution, differentiation, and repeated applications of the Chain Rule. As a result we have that the Laplacian in the Poincaré Disk model is given by

$$\Delta u = 8\frac{\partial^2 u}{\partial \rho^2} + + \left(\frac{4(\tanh^2(\rho/2)+1)}{\tanh(\rho/2)}\right)\frac{\partial u}{\partial \rho} + \left(\frac{2}{\sinh^2(\rho/2)\cosh^2(\rho/2)}\right)\frac{\partial^2 u}{\partial \sigma^2}. \tag{5.5}$$

Just as in Section 5.1, we can use separation of variables on this expression to find the eigenvalues. We once again assume that a function F can be separated into a function of each variable. Then $F(\rho, \sigma) = T(\rho)G(\sigma)$ and we solve for each function independently. The derivation is in Appendix D and includes a change of variables in order to get one of the resulting equations in a more well known form. The method in Appendix D is exactly the same as in Appendix B.

The function $G(\sigma)$ ends up being exactly the same as the function $\Theta(\theta)$ from the Euclidean case in Section 5.1, though with a different constant, denoted μ^2. Since the equations are otherwise identical, μ must take the same values as k, so $\mu = 0, 1, 2, 3, \cdots$. Once again, we can use each value of μ to find a solution for $T(\rho)$. The functions $T(\rho)$ are similar to $R(r)$ in that $T(\rho)$ also belong to a known class of functions. Solutions for $T(\rho)$ are Associated Legendre functions, which are similar to Bessel functions, and values for λ in this case are the zeros of the Associated Legendre functions. Analogous to the Euclidean case, the eigenvalues of F are also zeros of these Associated Legendre functions. Unfortunately, Associated Legendre functions of non-integer order are complex valued functions whose zeros are often complex valued as well [18, p. 581]. In general, $T(\rho)$ will be an Associated Legendre function of non-integer order and so will have complex valued zeros. However, the eigenvalues of F must, by definition, be positive real numbers. So mimicking the approach that we took in the Euclidean case would require a deeper understanding of the zeros of Associated Legendre functions than we needed for Bessel functions. Hence we look for a different approach which does not involve explicit calculation of the eigenvalues of hyperbolic domains. However, it can involve calculating explicit eigenvalues of Euclidean disks since we showed that this was feasible in Section 5.1. To begin, we examine hyperbolic triangles in depth and look for a Euclidean domain related to a given triangle.

6 Hyperbolic Triangles

In order to understand the fundamental gap for hyperbolic triangles, we must first understand hyperbolic triangles. In particular, we are interested in when these triangles exist and in the relationships between sides and angles. Recall that we also intend to bound these triangles with both an inscribed and a circumscribed circle. Thus we must know if and when these circles exist and how to find their radii. We first present a condition for the existence of a hyperbolic triangle and a simple relationship between the sides and angles. We then present conditions for the existence of inscribed and circumscribed circles as well as formulae for their radii.

6.1 Introduction and Existence

Euclidean triangles are simple to distinguish from other polygons: they have 3 straight line sides that create 3 distinct vertices and form 3 interior angles while enclosing a region of the Euclidean plane. Recall that in Euclidean geometry, straight lines are the geodesics. As with Euclidean triangles, hyperbolic triangles are formed by three geodesics that create 3 distinct vertices, form 3 interior angles and enclose a region of the Poincaré Disk. In general, hyperbolic triangles have an appearance like the triangle shown in Figure 7. Every hyperbolic triangle has at least one side that is not a diameter of the bounding circle and hence has at least one side that is a portion of an arc. In terms of their geodesic sides, hyperbolic and Euclidean triangles are similar. However, in terms of angles, they are very different. We recall that every triangle in Euclidean geometry has three angles and that their sum must be equal to π. Hyperbolic triangles also have 3 angles, but instead of summing to π, they must sum to less than π [3]. In fact, there exists a hyperbolic triangle with angles α, β, and γ if and only if $\alpha + \beta + \gamma < \pi$. This is a necessary and sufficient, as well as simple, condition for determining the existence of a hyperbolic triangle. Notice that the condition depends only on the angles and so we will look to formulate the rest of this section in terms of the angles of a hyperbolic triangle.

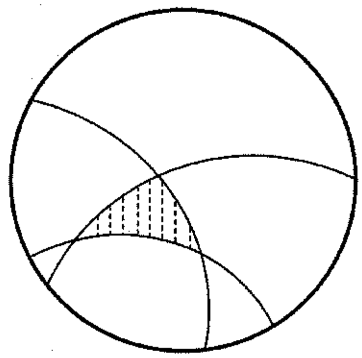

Figure 7: We see a typical hyperbolic triangle inside the Poincaré Disk model. The three sides are portions of arcs that meet the boundary circle at right angles and thus are geodesics. The dotted line region enclosed by the three geodesics is the hyperbolic triangle.

6.2 Relationship Between Sides and Angles

There are many useful relationships known about triangles in Euclidean geometry. Two of the most well known relationships are the law of sines and law of cosines. They are two ways of expressing a relationship between the sides and angles of Euclidean triangles. There are hyperbolic analogues of both of these laws and here we focus on the law of cosines [11, p. 495]. Consider any hyperbolic triangle with angles α, β, and γ and corresponding sides a, b, and c, so that angle α opens into side a, angle β opens into side b, angle γ opens into side c, as shown in Figure 8.

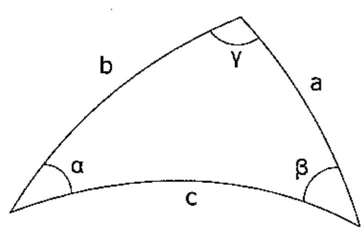

Figure 8: The labeling of the sides and angles for a hyperbolic triangle. By convention, we denote the lengths of the sides opposite angles α, β, and γ, by a, b, and c respectively.

Then the hyperbolic law of cosines is given by

$$\cosh(a) = \cosh(b)\cosh(c) - \sinh(b)\sinh(c)\cos(\alpha).$$

Unfortunately, this law is more useful when the side lengths are known. We are looking for a relationship that can determine the side lengths from the angles. Fortunately, there is a corollary to the hyperbolic law of cosines that states

$$\cosh(a) = \frac{\cos(\beta)\cos(\gamma) + \cos(\alpha)}{\sin(\beta)\sin(\gamma)}. \tag{6.1}$$

There are analogous equations for determining $\cosh(b)$ and $\cosh(c)$. This is precisely the relationship that we seek, giving us information about the side lengths based entirely on the angles. Notice that since $\cosh(a)$ depends only on the angles, once the angles are determined, the length of side a is determined. Using the two analogous equations, we notice that all three side lengths are determined by the angles and thus the entire triangle is determined by the three angles. This is strikingly different from Euclidean geometry where knowing the three angles will give us a ratio between the side lengths, but no exact side lengths. However, this is exactly what we were hoping for, since knowing the three angles of a hyperbolic triangle completely determines the triangle.

6.3 Inscribed Circles

We now turn our attention to the inscribed and circumscribed circles of hyperbolic triangles, beginning with inscribed circles. An *inscribed circle* of a polygon is defined to be the unique circle that is tangent to each side of the polygon, as shown in Figure 9.

In Euclidean geometry, every triangle has an inscribed circle and it turns out the same is true in hyperbolic geometry. Thus, regardless of the three angles,

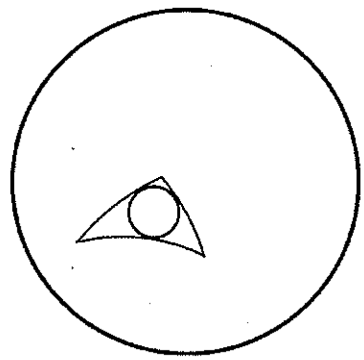

Figure 9: The inscribed circle is the unique circle contained within the triangle and tangent to each side of the triangle.

an inscribed circle will always exist. Furthermore, Beardon [3, p. 249] gives us a formula for the radius of the inscribed circle, which we denote r_I, that depends only on the angle measures of the triangle. We have that

$$\tanh^2(r_I) = \frac{\cos^2(\alpha) + \cos^2(\beta) + \cos^2(\gamma) + 2\cos(\alpha)\cos(\beta)\cos(\gamma) - 1}{2(1+\cos(\alpha))(1+\cos(\beta))(1+\cos(\gamma))}. \quad (6.2)$$

Thus we have everything we need concerning inscribed circles since they always exist and we have an explicit formula for the radius that depends only on the angles of the triangle.

6.4 Circumscribed Circles

The final geometric shape that we need is the circumscribed circle to our hyperbolic triangle. A *circumscribed circle* is defined as the circle that passes through the three vertices of a triangle as shown in Figure 10.

Since three points determine a unique circle, each circumscribed circle is unique. As with inscribed circles, every Euclidean triangle has a circumscribed circle. However, the same is not true for hyperbolic triangles. According to Fenchel [8, p. 118], a hyperbolic triangle with angles α, β, and γ and sides a, b,

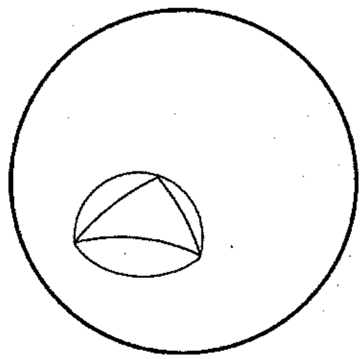

Figure 10: The circumscribed circle is the unique circle containing the triangle and passing through each of the vertices of the triangle.

and c has a circumscribed circle only if each of

$$\sinh\left(\frac{a}{2}\right), \quad \sinh\left(\frac{b}{2}\right), \quad \sinh\left(\frac{c}{2}\right), \tag{6.3}$$

is less than the sum of the other two. Using the relation

$$\sinh^2\left(\frac{x}{2}\right) = \frac{\cosh(x) - 1}{2},$$

combined with Eq. (6.1), we can reformulate the condition to be entirely in terms of angles. Indeed, for side a, we have

$$\sinh\left(\frac{a}{2}\right) = \sqrt{\frac{\cosh(a) - 1}{2}} = \sqrt{\frac{\cos(\beta)\cos(\gamma) + \cos(\alpha) - \sin(\beta)\sin(\gamma)}{2\sin(\beta)\sin(\gamma)}}, \tag{6.4}$$

with two similar expressions for the sides b and c. Thus we have criteria for the existence of a circumscribed circle of a hyperbolic triangle in terms of only the angles of the triangle. Additionally, Fenchel [8, p. 119] provides an explicit formula for the radius of the circumscribed circle, which we denote r_C. Letting

$2\Sigma = \alpha + \beta + \gamma$, we have

$$\tanh^2(r_C) = \frac{\cos(\Sigma)}{\cos(\Sigma - \alpha)\cos(\Sigma - \beta)\cos(\Sigma - \gamma)}. \tag{6.5}$$

Thus we have an equation for the radius of the circumscribed circle in terms of the angles of the triangle as well.

So given any three angles, we can determine whether or not there is a hyperbolic triangle with those angles. If there is, then we can determine if there is a circumscribed circle. If one does exist, then we can find the radii of both the inscribed and circumscribed circles. All of this information is determined completely by the original three angles. Now that we can determine the bounding circles, we need to find the eigenvalues of the disks they bound and relate those eigenvalues to the eigenvalues of the triangle, which we do in the next section.

7 Eigenvalues of Euclidean Disks

The Dirichlet eigenvalues of disks in the Euclidean plane have been well studied. Euclidean disks are one of the few regions whose Dirichlet eigenvalues can be calculated explicitly. In particular, the eigenvalues of Euclidean disks are the zeros of a class of functions known as Bessel Functions. In this section, we discuss Bessel Functions, their properties, and how they relate to the eigenvalues of Euclidean disks.

7.1 Bessel Functions

Bessel functions are a type of cylinder function that often arise in boundary value problems on cylindrical domains [13, pp. 99-103]. A cylinder function is any function $u(z)$ which satisfies the differential equation

$$u'' + \frac{1}{z}u' + \left(1 - \frac{\nu^2}{z^2}\right)u = 0, \tag{7.1}$$

where z is a complex variable and ν is a parameter that can be either real or complex. This equation is known as Bessel's equation of order ν and thus the solution, J_ν, is known as the Bessel function of order ν. The easiest type of Bessel equation to solve is one for which ν is a non-negative integer. Indeed, if $\nu = n$ is a non-negative integer then the Bessel function of order n can be given explicitly by

$$J_n(z) = \sum_{k=0}^{\infty} \frac{(-1)^k (z/2)^{(n+2k)}}{k!(n+k)!}. \tag{7.2}$$

Functions of the type (7.2) are known as Bessel functions of the first kind of order n. These functions satisfy the following recurrence relations for all n

$$J_{n-1}(z) + J_{n+1}(z) = \frac{2n}{z} J_n(z),$$

$$J_{n-1}(z) - J_{n+1}(z) = 2J_n'(z),$$

as well as the relations

$$\frac{d}{dz}\left(z^n J_n(z)\right) = z^n J_{n-1}(z), \qquad \forall n. \tag{7.3}$$

$$\frac{d}{dz}\left(z^{-n} J_n(z)\right) = -z^{-n} J_{n+1}(z), \qquad \forall n. \tag{7.4}$$

We will be most interested in the Bessel functions of the first kind of orders 0 and 1. All further mention of Bessel functions refers to Bessel functions of the first kind unless otherwise stated. These two functions can be written explicitly (though we omit that here) and can be used to define all Bessel functions with non-negative integer order greater than 1. Of more interest to us is the fact that the zeros of Bessel functions are known to be the eigenvalues of the unit disk in the Euclidean plane. We are interested in the first two eigenvalues of Euclidean disks and the next sections show exactly which zeros of which Bessel functions correspond to those eigenvalues.

7.2 First Eigenvalue of a Euclidean Disk

Though all of the Dirichlet eigenvalues of Euclidean disks have been studied, particular attention has been paid to the first eigenvalue. It has become a standard result that the first eigenvalue of a Euclidean ball of radius 1 in n dimensions is the square of the first zero of the Bessel function of order $\left(\frac{n}{2}-1\right)$ [7, p. 293]. Since the disks that we are concerned with arise in 2 dimensions, we set $n = 2$. Thus we are interested in the Bessel function of order 0, J_0. In particular, we are interested in the first zero of this function, denoted j_0, and its square, $(j_0)^2$. Since there is no known explicit representation of the zeros of Bessel functions, we use Mathematica to find a numerical approximation. However, (j_0^2) is the first eigenvalue for a disk of radius 1 and we would like to know the eigenvalue of a disk with any radius. The eigenvalues for a disk of radius r scale by a factor of $\frac{1}{r^2}$. That is, if λ_1^2 is the first eigenvalue of the unit disk, then $\frac{(\lambda_1^2)}{(r^2)}$ is the first eigenvalue of the disk of radius r [1, p. 1056]. Thus we have an approximation for the first eigenvalue of a Euclidean disk of radius r. Note that our numerical approximation can be given with arbitrarily high precision.

7.3 Second Eigenvalue of a Euclidean Disk

Finding the second eigenvalue proves to be slightly more difficult, though it is still a matter of determining which zero of which Bessel function is the next eigenvalue. Since we are considering the eigenvalues in ascending order, all we must determine is which zero of which Bessel function is the next largest after the first zero of J_0. Fortunately, Bessel functions possess a nice property from which our answer will follow.

Lemma: The zeros of Bessel functions interlace. That is, if j_n^i denotes the i^{th} zero of the Bessel function of order n, then

$$0 < j_n^1 < j_{n+1}^1 < j_n^2 < j_{n+1}^2 \cdots \quad \text{for } i \in \mathbb{Z}, i \geq 1. \tag{7.5}$$

Proof: Recall from Eq. (7.3) that the following relation holds for $z \in \mathbb{C}$ and for all n,

$$\frac{d}{dz}\left(z^n J_n(z)\right) = z^n J_{n-1}(z).$$

We restrict our attention to $z \in \mathbb{R}$ since the Bessel functions and their zeros that arise in our setting are always real valued. We now apply Rolle's theorem to the relation. Rolle's theorem states that for any real-valued function f that is continuous on a closed interval $[a, b]$ and differentiable on the open interval (a, b) with $f(a) = f(b)$, then there exists a point $c \in (a, b)$ such that $f'(c) = 0$. Since Bessel functions and the function z^n are both real-valued, continuous, and differentiable everywhere, Rolle's theorem applies to $z^n J_n$ for all n. So let $a = j_n^i$ and $b = j_n^{i+1}$. Then by Rolle's theorem, there exists a point c with $c \in (j_n^i, j_n^{i+1})$ such that $\frac{d}{dz}\left(c^n J_n(c)\right) = 0$. However, by the relation above, $\frac{d}{dz}\left(z^n J_n(z)\right) = z^n J_{n-1}(z)$, so $c^n J_{n-1}(c) = 0$. Since $0 < j_n^i < c$, we have $c > 0$ and so $c^n > 0$ as well. Thus $c^n J_{n-1}(c) = 0$ implies $J_{n-1}(c) = 0$ so that c is a zero of J_{n-1}. Then $c \in (j_n^i, j_n^{i+1})$ is a zero of J_{n-1} implying that between any two zeros of J_n is a zero of J_{n-1}.

Replacing n with $n-1$ in Eq. (7.4), we obtain the relation

$$\frac{d}{dz}\left(z^{-(n-1)}J_{n-1}(z)\right) = -z^{-(n-1)}J_n(z).$$

Repeating the same argument above using this relation shows that between any two zeros of J_{n-1} is a zero of J_n. Thus the zeros interlace and listing them in ascending order gives the desired result. □

In Figure 11, we see the first several Bessel functions plotted. From the graphs, it is apparent that the zeros of the Bessel functions interlace, verifying that Lemma 7.3 holds. In particular, we see that between any two zeros of J_0 is a zero of J_1 and so the first zero of J_1 is smaller than the second zero of J_0. Thus the second eigenvalue of the Euclidean disk must be the first zero of the Bessel function of order 1 rather than the second zero of the Bessel function of order 0. Once again, we can use Mathematica to numerically find this value to any precision and, as with the first eigenvalue, it scales by a factor of $\frac{1}{r^2}$. Note that these are eigenvalues for Euclidean disks, not hyperbolic disks. However, as the eigenvalues of hyperbolic disks are not easy to calculate explicitly, we will instead use the eigenvalues of the Euclidean disks to bound the eigenvalues of the hyperbolic disk.

8 An Upper Bound for the Fundamental Gap for Hyperbolic Triangles

We are finally ready to examine the fundamental gap for a hyperbolic triangle. In the first section, we present the skeleton of the argument that leads to an upper bound and in the second and third sections, we provide the details.

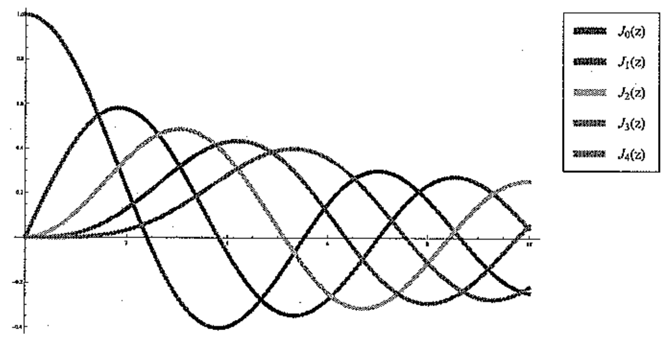

Figure 11: We see the graphs of the first five Bessel functions. We can clearly see the interlacing of the zeros for consecutive functions. In particular, the first non-trivial zero of J_1 (blue) is less than the second zero of J_0 (red).

8.1 Towards an Upper Bound

The upper bound for the fundamental gap for a hyperbolic triangle will depend on the eigenvalues of the inscribed and circumscribed disks, as well as on the eigenvalues of the Euclidean disks with the same radii. So for any hyperbolic triangle T with inscribed circle I and circumscribed circle C, define

λ_l^T : the eigenvalues of the triangle T we are interested in,

λ_l^I : the eigenvalues of the disk whose boundary is the inscribed circle of T,

λ_l^C : the eigenvalues of the disk whose boundary is the circumscribed circle of T.

Recall that in Section 2.2, we discussed the concept of domain monotonicity in the Euclidean plane. It turns out that every Riemannian manifold has the same domain monotonicity property [6, pp. 17-18]. Since the Poincaré Disk is indeed a Riemannian manifold (it behaves like $\mathbb{R}^n$ in small patches), we can apply domain monotonicity to regions in the Poincaré Disk. In particular, applying domain monotonicity to the triangle and the two bounding disks, we see that since $I \subseteq T \subseteq C$ we have

$$\lambda_1^I \geq \lambda_1^T \geq \lambda_1^C \quad \text{and} \quad \lambda_2^I \geq \lambda_2^T \geq \lambda_2^C. \tag{8.1}$$

The fundamental gap for T is $\lambda_2^T - \lambda_1^T$. From the inequality on the right in Eq. (8.1), we see that $\lambda_2^I \geq \lambda_2^T$. From the inequality on the left, we have that $\lambda_1^T \geq \lambda_1^C$ which implies that $-\lambda_1^C \geq -\lambda_1^T$. Then, adding these two inequalities, we obtain the upper bound

$$\lambda_2^T - \lambda_1^T \leq \lambda_2^I - \lambda_1^C. \tag{8.2}$$

In a similar fashion, we can obtain a lower bound for the fundamental gap, though we will focus on the upper bound. Notice that we have to be careful in our use of domain monotonicity; the upper bound depends on one eigenvalue from each of the disks and not both eigenvalues from one of the disks. Considering Equation (8.2), all we need now is information about λ_2^I and λ_1^C and we will have information about the fundamental gap for the triangle. In particular, if we have an upper bound for λ_2^I and a lower bound for λ_1^C, then we have an upper bound for the quantity $\lambda_2^I - \lambda_1^C$, and hence an upper bound for the fundamental gap for T. The next sections will provide the details of finding an upper bound for λ_2^I and a lower bound for λ_1^C.

8.2 Ratio of Eigenvalues

We begin with finding an upper bound for λ_2^I. In their investigations of the second eigenvalue of general hyperbolic domains, Benguria and Linde [4, pp. 245-247] provide some results that relate the eigenvalues of Euclidean and hyperbolic domains. In particular, they have two main results and a direct consequence of one of them is the relationship that we seek. The result is as follows. Let $\lambda_i^H(\delta)$ be the i[th] Dirichlet eigenvalue of the hyperbolic geodesic ball of radius δ. Then

$$\frac{\lambda_2^H(\delta)}{\lambda_1^H(\delta)} \tag{8.3}$$

is a strictly decreasing function of δ. Thus as $\delta \to \infty$, we have $\lambda_2^H(\delta)/\lambda_1^H(\delta) \to 1$. However, the limiting case as $\delta \to 0$ is also of interest. In particular, as δ decreases, a hyperbolic disk and a Euclidean disk of radius δ begin to look the same. This is a result of the way in which distances are skewed in the Poincaré Disk and smaller areas are impacted by the skewing less. So as the area of a domain approaches 0, the hyperbolic domain and its Euclidean counterpart look increasingly more alike. In fact, if B_E and B_H are respectively the Euclidean and hyperbolic balls of radius δ, then $\lim_{\delta \to 0} B_H = B_E$. Letting $\lambda_i^B(\delta)$ be the Dirichlet eigenvalues of a Euclidean ball of radius δ, it follows from the result of Benguria and Linde [4] that

$$\frac{\lambda_2^H(\delta)}{\lambda_1^H(\delta)} < \lim_{\delta \to 0}\left(\frac{\lambda_2^H(\delta)}{\lambda_1^H(\delta)}\right) = \frac{\lambda_2^B(\delta)}{\lambda_1^B(\delta)}, \tag{8.4}$$

since $\lambda_2^H(\delta)/\lambda_1^H(\delta)$ decreases as δ increases. Thus Eq. (8.4) tells us that the ratio of the first two eigenvalues of a hyperbolic ball of radius δ is less than the ratio of the first two eigenvalues of a Euclidean ball of radius δ. Additionally, since the Euclidean ball is the limiting case of the hyperbolic ball, this upper bound is optimal.

Returning to our hyperbolic triangle T, if we define

λ_l^E : the eigenvalues of the Euclidean disk whose boundary is the circle of the same radius as the inscribed circle of T and use the same definitions from Section 8.1, then Eq. (8.4) tells us that

$$\frac{\lambda_2^I}{\lambda_1^I} \leq \frac{\lambda_2^E}{\lambda_1^E}. \tag{8.5}$$

Recall that in Section 7, we found approximate values for the first two eigenvalues of a Euclidean disk of arbitrary radius. In particular, we can find approximate values for both λ_2^E and λ_1^E. Thus we know the ratio $\frac{\lambda_2^E}{\lambda_1^E}$. Letting $\frac{\lambda_2^E}{\lambda_1^E} = K$, we have that $\frac{\lambda_2^I}{\lambda_1^I} \leq K$ and hence

$$\lambda_2^I \leq K\lambda_1^I. \tag{8.6}$$

Since we can determine K, which is approximately $K \approx (3.83/2.40)^2 \approx 2.55$, we can find an upper bound for λ_2^I by finding an upper bound on λ_1^I. Thus we need an upper bound for λ_1^I and a lower bound for λ_1^C.

8.3 Upper Bound for λ_1^I and Lower Bound for λ_1^C

We begin with an upper bound for λ_1^I. Fortunately, the first eigenvalue of a general hyperbolic disk has been well studied over the years and an upper bound is known. The classic result from Cheng [7, p. 294] states that for a hyperbolic disk of radius r,

$$\lambda_1^I \leq \frac{1}{4} + \left(\frac{2\pi}{r}\right)^2. \tag{8.7}$$

Thus if we know the radius of the inscribed disk, we have an upper bound for λ_1^I. Since we can determine the radius of the inscribed disk from Eq. (6.2), we have an upper bound for λ_1^I.

Finally, we turn to finding a lower bound for λ_1^C. We discuss a lower bound in more general terms and then reduce to our case. Li and Yau [14, p. 215] provide a lower bound for the first eigenvalue for a general Riemannian manifold in n dimensions. Their bound depends on the dimension n of the manifold, the curvature κ of the manifold, the mean curvature H of the boundary of the manifold, and the radius i of the largest inscribed geodesic ball in the manifold. We discussed the curvature of the Poincaré Disk in Section 3.2 and the curvature of the boundary is similar in concept, though takes a different value. Then a lower bound for the first eigenvalue λ_1 of the manifold is given by

$$\lambda_1 \geq \frac{1}{\gamma}\left(\frac{1}{4(n-1)i^2}(\log(\gamma))^2 + (n-1)\kappa\right), \tag{8.8}$$

where

$$\gamma = \max\{e^{1+\sqrt{1-4(n-1)^2 i^2 \kappa}}, e^{-2(n-1)Hi}\}.$$

Now we can reduce to the case in which we are interested [14].

We are interested in reducing this to the case of the inscribed disk in a hyperbolic triangle. Thus we are in two dimensions so $n = 2$ and as before, $\kappa = -1$ in the Poincaré Disk. We need to know the radius of the largest geodesic ball that fits inside the disk. However, the geodesic balls of dimension 2 are simply disks and so the largest circle that fits inside a disk of radius r is the circle of radius r. So if r_I is the radius of the inscribed disk, we have $i = r_I$. Lastly, we need to consider γ and, in particular, the mean curvature of the boundary, H. By examining the proof of Li and Yau of the lower bound in Eq. (8.8), we see that H must be negative. However, the curvature of a circle (the boundary in our case) is always positive, so we cannot possibly be in the case where $\gamma = e^{-2(n-1)Hi}$. Thus we are in the case of $\gamma = e^{1+\sqrt{1-4(n-1)^2 i^2 \kappa}}$ and substituting $n = 2$, $i = r_I$, $\kappa = -1$, and γ into Eq. (8.8), we have

$$\lambda_1 \geq \frac{1}{e^{1+\sqrt{1+4r_I^2}}}\left(\frac{1}{4r_I^2}\left(1+\sqrt{1+4r_I^2}\right)^2 - 1\right). \tag{8.9}$$

Finally, we have obtained a lower bound for the first eigenvalue of a hyperbolic disk of any radius. Now we have the desired lower bound for λ_1^C and all of the necessary information to complete the upper bound for the fundamental gap for hyperbolic triangles.

Recall from Section 8.1 that we derived the following,

$$\lambda_2^T - \lambda_1^T \leq \lambda_2^I - \lambda_1^C.$$

Additionally, we showed that if $\frac{\lambda_2^E}{\lambda_1^E} = K$, then $\lambda_2^I \leq K\lambda_1^I$. Above, we determined an upper bound for λ_1^I and a lower bound for λ_1^C. Combining all of these facts, we have the following:

Theorem 1 (Upper Bound): Let T be a hyperbolic triangle with eigenvalues λ_i^T, an inscribed disk of radius r_I, and suppose that there exists a circumscribed circle of T. Let λ_i^E be the eigenvalues of a Euclidean disk with radius r_I and let $\frac{\lambda_2^E}{\lambda_1^E} = K$. Then

$$\lambda_2^T - \lambda_1^T \leq K\left(\frac{1}{4} + \left(\frac{2\pi}{r_I}\right)^2\right) - \frac{\left(\frac{1}{4r_I^2}\left(1+\sqrt{1+4r_I^2}\right)^2 - 1\right)}{e^{1+\sqrt{1+4r_I^2}}}. \tag{8.10}$$

Notice that this upper bound depends only on the radius of the inscribed circle r_I and the ratio of the first two eigenvalues of the Euclidean disk corresponding to the inscribed circle. However, Eq. (8.10) is not in a particularly nice form and so we investigate it numerically to find an upper bound that can be stated more simply.

9 Numerically Investigating the Upper Bound

In this section, we look to reduce the bound given in Eq. (8.10) to a more manageable form using numerical techniques and the following process. We generate three random angles, α, β, and γ, between 0 and $\pi/2$ radians and check to make sure that they form a hyperbolic triangle, i.e, that their sum is less than π. Let a, b, and c be the sides of the triangle opposite α, β, and γ respectively. Then we check that each of

$$\sinh\left(\frac{a}{2}\right), \quad \sinh\left(\frac{b}{2}\right), \quad \sinh\left(\frac{c}{2}\right)$$

is less than the sum of the other two, ensuring the existence of a circumscribed circle. Now we determine the radii of the inscribed and circumscribed circles using Eqs. (6.2) and (6.5). We then determine the first two eigenvalues of the Euclidean disk of the same radius as the inscribed circle, using Mathematica to find the first zero of the Bessel function of order 0 and the first zero of the Bessel function of order 1. Finally, we use Eqs. (8.7) and (8.9) to determine an upper bound for λ_1^I and a lower bound for λ_1^C and calculate an upper bound for the fundamental gap for our random triangle. Depending on the angles randomly chosen, the radius of the circumscribed circle may be complex valued. If that is the case, we simply ignore that triangle. By repeating this process, we can examine the upper bound for the fundamental gap and try to express the upper bound in a more desirable fashion.

After acquiring the data, we can examine it using a program such as Microsoft Excel. We can conjecture an upper bound and then test it against all of the data collected. Doing this for over 100,000 randomly generated triangles, we have the following conjecture.

Gap Conjecture for Hyperbolic Triangles: Let T be any hyperbolic triangle with angles between 0 and $\frac{\pi}{2}$ radians, an inscribed circle of radius r_I, and suppose there exists a circumscribed circle of T. If λ_i^T denotes the i$^{\text{th}}$ Dirichlet eigenvalue of T, then

$$\lambda_2^T - \lambda_1^T \leq 10.2 \left(\frac{\pi}{r_I}\right)^2. \tag{9.1}$$

In order to get an idea of how this conjecture compares to Theorem 1, we provide a comparison between the upper bound given by Eq. (8.10) and by Eq. (9.1) for ten distinct triangles in Table 1. We give the angles, the radius of the inscribed circle r_I, the upper bound for the fundamental gap provided by Eq. (8.10), the upper bound for the fundamental gap provided by Eq. (9.1), and the difference between the two values for each of the ten triangles. We see that triangles 1-6 all have a difference between the upper bounds of less than 4. Triangles 1, 2, and 3 are all equilateral, triangle 4 has three small angles, triangle 5 has three angles that are relatively close to each other, and triangle 6 has one large angle and two smaller angles. Triangles 7-10 have a difference between the two upper bounds of at least 16 and as large as 347. All of these triangles shares a common quality: they each have two angles greater than or equal to $\frac{\pi}{4}$, i.e. two large angles. In particular, notice that each of triangles 8, 9, and 10 have angles of $\frac{\pi}{2}$ and $\frac{\pi}{3}$. As the third angle increases and the sum of the three angles approaches π, the difference between the two upper bounds gets larger.

Since the angles determine the radius of the inscribed disk, we can find similar patterns in the relationship between the radius of the inscribed disk and the difference between the upper bounds. It is apparent from Table 1 that as r_I decreases, the bound given in the conjecture becomes larger and farther away from the upper bound given in Theorem 1. In fact, as $r_I \to 0$, we see that our conjecture states that the fundamental gap becomes unbounded. In Section 2.2, we mentioned that Lu and Rowlett showed that the fundamental gap is unbounded for collapsing triangles that have two angles α and β satisfying $\frac{2}{3} < \frac{\alpha}{\beta} < 1$. [15, p. 3]. Our conjecture provides somewhat of a hyperbolic analog for

Triangle	Angles	r_I	Theorem 1	Gap Conjecture	Difference
1	$\frac{\pi}{4}, \frac{\pi}{4}, \frac{\pi}{4}$	0.36	758.98	761.80	2.83
2	$\frac{\pi}{10}, \frac{\pi}{10}, \frac{\pi}{10}$	0.52	365.58	366.57	0.99
3	$\frac{\pi}{20}, \frac{\pi}{20}, \frac{\pi}{20}$	0.54	340.42	341.30	0.87
4	$\frac{\pi}{10}, \frac{\pi}{20}, \frac{\pi}{30}$	0.54	346.81	347.71	0.90
5	$\frac{\pi}{3}, \frac{\pi}{4}, \frac{\pi}{5}$	0.34	883.78	887.18	3.40
6	$\frac{\pi}{2}, \frac{\pi}{9}, \frac{\pi}{9}$	0.33	917.60	921.04	3.44
7	$\frac{\pi}{2}, \frac{\pi}{4}, \frac{\pi}{5}$	0.16	3939.49	3956.92	17.43
8	$\frac{\pi}{2}, \frac{\pi}{3}, \frac{\pi}{10}$	0.16	3730.15	3746.36	16.21
9	$\frac{\pi}{2}, \frac{\pi}{3}, \frac{\pi}{7}$	0.10	9189.64	9231.01	41.37
10	$\frac{\pi}{2}, \frac{\pi}{3}, \frac{\pi}{6.1}$	0.036	75953.4	76300.42	347.02

Table 1: We see the angles, inscribed radius r_I, upper bound for the fundamental gap from Eq. (8.10), the upper bound for the fundamental gap from Eq. (9.1), and the difference between the two values for ten triangles. Triangles that are close to equilateral or that have small angles minimize the difference between the two upper bounds. Triangles with larger angles tend to have a large difference between the two upper bounds.

this result in that the fundamental gap seems to be unbounded for a restricted class of collapsing hyperbolic triangles, though our restriction differs from that of Lu and Rowlett. Currently, we do not have a proof for this conjecture or an explanation as to the constant 10.2. Note that the form of our upper bound is comparable to the form of the original Fundamental Gap Conjecture, which can be rearranged to have the form $3\left(\frac{\pi}{d}\right)^2$. Additionally, the upper bound for the fundamental gap for the Schrödinger operator in Eq. (2.6) was also given in this form.

10 Conclusion

We have examined the Dirichlet eigenvalues of hyperbolic triangles and, in particular, the fundamental gap for these triangles. Using domain monotonicity along with the inscribed and circumscribed circles for a given hyperbolic triangle, we are able to find an upper bound for the fundamental gap for arbitrary hyperbolic triangles that have a circumscribed circle. We chose not to pursue an explicit numerical calculation of the eigenvalues of hyperbolic disks since they arise as the zeros of Associated Legendre functions. When dealing with arbitrary disks, we are likely to come across Associated Legendre functions of non-integral order which causes difficulty in determining the eigenvalues of a hyperbolic disk. As such, we chose to use a relationship between the eigenvalues of Euclidean and hyperbolic disks. Using known bounds on the eigenvalues of hyperbolic disks, we formulate an upper bound for the fundamental gap for hyperbolic triangles that have a circumscribed circle.

Once we obtained a preliminary upper bound for the fundamental gap, we further expanded on it by using numerical data to conjecture a simpler upper bound. There is much work left to be done concerning this upper bound. First of all, an explanation of the constant 10.2 is needed. We also do not know how sharp of a bound we have. Indeed, we have used a series of inequalities and we only know that one of the bounds is sharp, namely the bound on the ratio of the first two eigenvalues given in Eq. (8.4). Furthermore, our upper bound is only for a specific class of triangles. A logical next step would be to find a similar bound for arbitrary hyperbolic triangles or general polygons with more than three sides, though such bounds may require different techniques. Such upper bounds would be a step towards finding an upper bound for a general hyperbolic convex domain and a hyperbolic analog for van den Berg's original Fundamental Gap Conjecture. What we have provided is just the beginning of an understanding of the fundamental gap for triangles in hyperbolic geometry and there is much opportunity for further work.

References

[1] Ashbaugh, Mark S. and Benguria, Rafael D. *A Sharp Bound for the Ratio of the First Two Dirichlet Eigenvalues of a Domain in a Hemisphere of* $\mathbb{S}^n$. Trans. Amer. Math. Soc., 353 (2001), No. 3, 1055-1087.

[2] Bartle, Robert G. and Sherbert, Donald R. *Introduction to Real Analysis,* 3^{rd} *Ed.* 2000. John Wiley and Sons, New York.

[3] Beardon, A.F. *Hyperbolic Polygons and Fuchsian Groups.* J. London Math. Soc., 20 (1979), No. 2, 247-254.

[4] Benguria, Rafael D. and Linde, Helmut. *A Second Eigenvalue Bound for the Dirichlet Laplacian in Hyperbolic Space.* Duke Math. J., 140 (2007), No. 2, 245-279.

[5] Buser, Peter. *Geometry and Spectra of Compact Riemann Surfaces.* 1992. Birkhauser, Boston.

[6] Chavel, Isaac. *Eigenvalues in Riemannian Geometry.* 1984. Academic Press, New York.

[7] Cheng, Shui-Yuen. *Eigenvalue Comparison Theorems and Its Geometric Applications.* Math. Z., 143 (1975), 289-297.

[8] Fenchel, Werner. *Elementary Geometry in Hyperbolic Space.* 1989. De Gruyter Studies in Mathematics, New York.

[9] Gordon, Carolyn and Webb, Gordon. *You Can't Hear the Shape of a Drum.* Am. Sci., 84 (1996), 46-55.

[10] Gordon, Carolyn, Webb, Gordon, and Wolpert, Scott. *One Cannot Hear the Shape of a Drum.* Bull. Amer. Math. Soc., 27 (1992), 134-138.

[11] Greenberg, Marvin Jay. *Euclidean and Non-Euclidean Geometries.* 2008. W.H Freeman and Company, New York.

[12] Kac, Mark. *Can One Hear the Shape of a Drum?* Amer. Math. Monthly, 73 (1966), No. 4, 1-23.

[13] Lebedev, N.N. *Special Functions and Their Applications.* 1965. Prentice Hall, New Jersey.

[14] Li, Peter and Yau, Shing-Tung. *Estimates of Eigenvalues of a Compact Riemannian Manifold.* Proc. Sympos. Pure Math., 36 (1980), 205-239.

[15] Lu, Zhiqin and Rowlett, Julie. *The Fundamental Gap Conjecture for Polygonal Domains.* 2008. arXiv:0810.4937v2

[16] Ramsay, Arlan and Richtmyer, Robert. *Introduction to Hyperbolic Geometry.* 1995. Springer-Verlag, New York

[17] Reuter, Martin, Wolter, Franz-Erich, and Peinecke, Niklas. *Laplace-Beltrami spectra as "Shape-DNA" of surfaces and solids.* Computer-Aided Design, 38 (2006), 342-366.

[18] Spanier, Jerome and Oldham, Keith B. *An Atlas of Functions.* 1987. Hemisphere, Washington.

[19] Stewart, James. *Multivariable Calculus,* 5^{th} *Ed.* 2003. Brooks/Cole, Belmont, California.

[20] van den Berg, Michiel. *On Condensation in the Free-Boson Gas and the Spectrum of the Laplacian.* J. Stat. Phys., 31 (1983), No. 3, 623-637.

[21] Singer, I.M, Wong, Bun, Yau Shing-Tung, and Yau, Stephen S.-T. *An estimate of the gap of the first two eigenvalues in the Schrödinger operator.* Ann. Scuola Norm. Sup. Pisa Cl. Sci. 4, 12 (1985), No. 2, 319-333.

A Derivation of the Laplacian in Polar Coordinates

We would like to translate the expression for the Laplacian

$$\Delta u = \frac{\partial^2 u}{\partial x^2} + \frac{\partial^2 u}{\partial y^2}, \tag{A.1}$$

into polar coordinates, using the relations

$$\begin{aligned} x &= r\cos(\theta), \\ y &= r\sin(\theta), \\ \theta &= \tan^{-1}\left(\frac{y}{x}\right), \\ x^2 + y^2 &= r^2. \end{aligned}$$

We begin by computing the partial derivatives of r with respect to x and y. We have that

$$\begin{aligned} \frac{\partial r}{\partial x} &= \frac{\partial}{\partial x}\left(\sqrt{x^2+y^2}\right) = \frac{2x}{2\sqrt{x^2+y^2}} = \frac{x}{\sqrt{x^2+y^2}} = \frac{x}{r} = \frac{r\cos(\theta)}{r} = \cos(\theta), \\ \frac{\partial r}{\partial y} &= \frac{\partial}{\partial y}\left(\sqrt{x^2+y^2}\right) = \frac{2y}{2\sqrt{x^2+y^2}} = \frac{y}{\sqrt{x^2+y^2}} = \frac{y}{r} = \frac{r\sin(\theta)}{r} = \sin(\theta). \end{aligned}$$

We will also need the partial derivatives of θ with respect to x and y, which are

$$\begin{aligned} \frac{\partial \theta}{\partial x} &= \frac{\partial}{\partial x}\left(\tan^{-1}\left(\frac{y}{x}\right)\right) = \frac{-y}{x^2(1+y^2/x^2)} = \frac{-r\sin(\theta)}{r^2} = \frac{-\sin(\theta)}{r}, \\ \frac{\partial \theta}{\partial y} &= \frac{\partial}{\partial}\left(\tan^{-1}\left(\frac{y}{x}\right)\right) = \frac{x}{x^2(1+y^2/x^2)} = \frac{r\cos(\theta)}{r^2} = \frac{\cos(\theta)}{r}. \end{aligned}$$

Next we wish to find $\frac{\partial^2 u}{\partial x^2}$ and $\frac{\partial^2 u}{\partial y^2}$. For this, we need the Chain Rule

$$\frac{\partial u}{\partial x} = \frac{\partial u}{\partial r}\frac{\partial r}{\partial x} + \frac{\partial u}{\partial \theta}\frac{\partial \theta}{\partial x}. \tag{A.2}$$

Using Eq. A.2, we see that

$$\frac{\partial^2 u}{\partial x^2} = \frac{\partial}{\partial x}\left(\frac{\partial u}{\partial x}\right) = \frac{\partial}{\partial x}\left(\frac{\partial u}{\partial r}\frac{\partial r}{\partial x} + \frac{\partial u}{\partial \theta}\frac{\partial \theta}{\partial x}\right) = \frac{\partial}{\partial x}\left(\frac{\partial u}{\partial r}\cos(\theta) - \frac{\partial u}{\partial \theta}\frac{\sin(\theta)}{r}\right),$$
$$\frac{\partial^2 u}{\partial y^2} = \frac{\partial}{\partial y}\left(\frac{\partial u}{\partial y}\right) = \frac{\partial}{\partial y}\left(\frac{\partial u}{\partial r}\frac{\partial r}{\partial y} + \frac{\partial u}{\partial \theta}\frac{\partial \theta}{\partial y}\right) = \frac{\partial}{\partial y}\left(\frac{\partial u}{\partial r}\sin(\theta) + \frac{\partial u}{\partial \theta}\frac{\cos(\theta)}{r}\right).$$

From these two expressions, we again apply the Chain Rule (Eq. A.2) to obtain the expressions

$$\begin{aligned}
\frac{\partial^2 u}{\partial x^2} &= \frac{\partial r}{\partial x}\frac{\partial}{\partial r}\left(\frac{\partial u}{\partial r}\cos(\theta) - \frac{\partial u}{\partial \theta}\frac{\sin(\theta)}{r}\right) + \frac{\partial \theta}{\partial x}\frac{\partial}{\partial \theta}\left(\frac{\partial u}{\partial r}\cos(\theta) - \frac{\partial u}{\partial \theta}\frac{\sin(\theta)}{r}\right) \\
&= (\cos(\theta))\frac{\partial}{\partial r}\left(\frac{\partial u}{\partial r}\cos(\theta) - \frac{\partial u}{\partial \theta}\frac{\sin(\theta)}{r}\right) \\
&\quad + \left(\frac{-\sin(\theta)}{r}\right)\frac{\partial}{\partial \theta}\left(\frac{\partial u}{\partial r}\cos(\theta) - \frac{\partial u}{\partial \theta}\frac{\sin(\theta)}{r}\right) \\
&= (\cos(\theta))\left(\frac{\partial^2 u}{\partial r^2}\cos(\theta) + \frac{\partial u}{\partial \theta}\frac{\sin(\theta)}{r^2} - \frac{\partial u}{\partial r \partial \theta}\frac{\sin(\theta)}{r}\right) \\
&\quad - \left(\frac{\sin(\theta)}{r}\right)\left(\frac{\partial u}{\partial r}(-\sin(\theta)) + \frac{\partial u}{\partial \theta \partial r}\cos(\theta) - \frac{\partial u}{\partial \theta}\frac{\cos(\theta)}{r} - \frac{\partial^2 u}{\partial \theta^2}\frac{\sin(\theta)}{r}\right),
\end{aligned}$$

and

$$\begin{aligned}
\frac{\partial^2 u}{\partial y^2} &= \frac{\partial r}{\partial y}\frac{\partial}{\partial r}\left(\frac{\partial u}{\partial r}\sin(\theta) + \frac{\partial u}{\partial \theta}\frac{\cos(\theta)}{r}\right) + \frac{\partial \theta}{\partial y}\frac{\partial}{\partial \theta}\left(\frac{\partial u}{\partial r}\sin(\theta) + \frac{\partial u}{\partial \theta}\frac{\cos(\theta)}{r}\right) \\
&= (\sin(\theta))\frac{\partial}{\partial r}\left(\frac{\partial u}{\partial r}\sin(\theta) + \frac{\partial u}{\partial \theta}\frac{\cos(\theta)}{r}\right) \\
&\quad + \left(\frac{\cos(\theta)}{r}\right)\frac{\partial}{\partial \theta}\left(\frac{\partial u}{\partial r}\sin(\theta) + \frac{\partial u}{\partial \theta}\frac{\cos(\theta)}{r}\right) \\
&= (\sin(\theta))\left(\frac{\partial^2 u}{\partial r^2}\sin(\theta) - \frac{\partial u}{\partial \theta}\frac{\cos(\theta)}{r^2} + \frac{\partial u}{\partial r \partial \theta}\frac{\cos(\theta)}{r}\right) \\
&\quad + \left(\frac{\cos(\theta)}{r}\right)\left(\frac{\partial u}{\partial r}\cos(\theta) + \frac{\partial u}{\partial \theta \partial r}\sin(\theta) - \frac{\partial u}{\partial \theta}\frac{\sin(\theta)}{r} + \frac{\partial^2 u}{\partial \theta^2}\frac{\cos(\theta)}{r}\right).
\end{aligned}$$

Then adding the two expressions above and grouping like terms gives

$$
\begin{aligned}
\left(\frac{\partial^2 u}{\partial x^2}+\frac{\partial^2 u}{\partial y^2}\right) &= \frac{\partial^2 u}{\partial r^2}\left(\sin^2(\theta)+\cos^2(\theta)\right)\\
&\quad+\frac{\partial^2 u}{\partial \theta^2}\left(\frac{\cos^2(\theta)}{r^2}+\frac{\sin^2(\theta)}{r^2}\right)+\frac{\partial u}{\partial r}\left(\frac{\sin^2(\theta)}{r}+\frac{\cos^2(\theta)}{r}\right)\\
&\quad+\frac{\partial u}{\partial \theta}\left(\frac{\sin(\theta)\cos(\theta)}{r^2}+\frac{\sin(\theta)\cos(\theta)}{r}-\frac{\sin(\theta)\cos(\theta)}{r^2}-\frac{\sin(\theta)\cos(\theta)}{r}\right)\\
&\quad+\frac{\partial u}{\partial r\partial \theta}\left(-\frac{\sin(\theta)\cos(\theta)}{r}+\frac{\sin(\theta)\cos(\theta)}{r}\right)\\
&\quad+\frac{\partial u}{\partial \theta\partial r}\left(-\frac{\sin(\theta)\cos(\theta)}{r}+\frac{\sin(\theta)\cos(\theta)}{r}\right)\\
&=\frac{\partial^2 u}{\partial r^2}(1)+\frac{\partial^2 u}{\partial \theta^2}\left(\frac{1}{r^2}\right)+\frac{\partial u}{\partial r}\left(\frac{1}{r}\right)+\frac{\partial u}{\partial \theta}(0)+\frac{\partial u}{\partial r\partial \theta}(0)+\frac{\partial u}{\partial \theta\partial r}(0)\\
&=\frac{\partial^2 u}{\partial r^2}+\left(\frac{1}{r}\right)\frac{\partial u}{\partial r}+\left(\frac{1}{r^2}\right)\frac{\partial^2 u}{\partial \theta^2}.
\end{aligned}
$$

Thus we see that the Laplacian in polar coordinates is

$$
\Delta u=\left(\frac{\partial^2 u}{\partial x^2}+\frac{\partial^2 u}{\partial y^2}\right)=\frac{\partial^2 u}{\partial r^2}+\left(\frac{1}{r}\right)\frac{\partial u}{\partial r}+\left(\frac{1}{r^2}\right)\frac{\partial^2 u}{\partial \theta^2}. \tag{A.3}
$$

B Separation of Variables for the Euclidean Polar Laplacian

We know the expression for the Laplacian in polar coordinates (Eq. (A.3)). We wish to solve the equation $\Delta F+\lambda F=0$. Now assume that $F(r,\theta)$ can be separated into two functions, each dependent on only one variable, so that

$F(r, \theta) = R(r)\Theta(\theta)$. Applying Δ to F, we see that

$$\begin{aligned}\Delta F &= \Delta R(r)\Theta(\theta)\\ &= \frac{\partial^2}{\partial r^2}\left(R(r)\Theta(\theta)\right) + \left(\frac{1}{r}\right)\frac{\partial}{\partial r}\left(R(r)\Theta(\theta)\right) + \left(\frac{1}{r^2}\right)\frac{\partial^2}{\partial \theta^2}\left(R(r)\Theta(\theta)\right)\\ &= R''(r)\Theta(\theta) + \left(\frac{1}{r}\right)R'(r)\Theta(\theta) + \left(\frac{1}{r^2}\right)R(r)\Theta''(\theta).\end{aligned}$$

where prime notation denotes differentiation with respect to the variable in which the function is given. Then

$$\begin{aligned}\Delta F + \lambda F = R''(r)\Theta(\theta) + \left(\frac{1}{r}\right)R'(r)\Theta(\theta)\\ + \left(\frac{1}{r^2}\right)R(r)\Theta''(\theta) + \lambda R(r)\Theta(\theta) = 0.\end{aligned} \tag{B.1}$$

Grouping terms, we have that

$$\Theta(\theta)\left(R''(r) + \left(\frac{1}{r}\right)R'(r) + \lambda R(r)\right) + \left(\frac{1}{r^2}\right)R(r)\Theta''(\theta) = 0. \tag{B.2}$$

Then putting all terms involving R on the left and all terms involving Θ on the right, we have

$$\frac{r^2R''(r) + rR'(r) + \lambda r^2 R(r)}{R(r)} = -\frac{\Theta''(\theta)}{\Theta(\theta)}. \tag{B.3}$$

Since the left side is only dependent on R and the right side only dependent on Θ, they must both equal a constant, which we label k^2. Setting each side equal to k^2 and rearranging gives the following set of equations,

$$\Theta''(\theta) + k^2\Theta(\theta) = 0, \tag{B.4}$$

$$r^2R''(r) + rR'(r) + \{\lambda r^2 - k^2\}R(r) = 0. \tag{B.5}$$

Now we can solve each of these independently. Equation (B.4) is known to be the equation for the Laplacian on a sphere with eigenvalues k^2 for $k = 0, 1, 2, 3, \cdots$. Hence we have determined the values for k^2 and so we can solve Eq. (B.5) for each value of k^2. If we compare Eq. (B.5) to Eq. (7.1) (multiplied by z^2), we see that the of solution Eq. (B.5) is the Bessel function of order k, denoted J_k. Therefore, the solutions to Eq.(B.5) are $J_k(r\sqrt{\lambda})$ and the eigenvalues are the zeros of this function where we let j_k^i denote the i$^{\text{th}}$ zero of the Bessel function of order k. The eigenvalues of F are then simply the eigenvalues of R, since when solving for the eigenvalues of R we have already taken into account the eigenvalues of Θ through the choice of k. Hence the eigenvalues of F are j_k^i.

C Derivation of the Laplacian in the Poincaré Disk Model

Here we will find the Laplacian in polar coordinates for the Poincaré Disk model using a similar method as for the Euclidean case in Appendix A. It is well known that the metric tensor in the disk model is given by [11, p. 565]

$$ds^2 = \frac{4(dx^2 + dy^2)}{(1 - x^2 - y^2)^2}. \tag{C.1}$$

Then, using the transformations ([16, p. 210])

$$\begin{aligned} x &= \tanh(\rho/2)\cos(\sigma), \\ y &= \tanh(\rho/2)\sin(\sigma), \end{aligned} \tag{C.2}$$

we can solve for the Laplacian in polar coordinates. For brevity, we only include an overview of the process. We first compute the following derivatives

$$\begin{aligned}\frac{\partial x}{\partial \rho} &= \frac{\cos(\sigma)}{2\cosh^2(\rho/2)},\\ \frac{\partial x}{\partial \sigma} &= -\tanh(\sigma/2)\sin(\sigma),\\ \frac{\partial y}{\partial \rho} &= \frac{\sin(\sigma)}{2\cosh^2(\rho/2)},\\ \frac{\partial x}{\partial \sigma} &= \tanh(\sigma/2)\cos(\sigma).\end{aligned}$$

Using the Chain Rule (Eq. A.2), we can compute $\partial u/\partial \rho$ and $\partial u/\partial \sigma$. Then we can use the elimination method to solve the system of equations and find that

$$\begin{aligned}\frac{\partial u}{\partial x} &= \left(2\cos(\sigma)\cosh^2(\rho/2)\right)\frac{\partial u}{\partial \rho} - \left(\frac{\sin(\sigma)}{\tanh(\rho/2)}\right)\frac{\partial u}{\partial \sigma},\\ \frac{\partial u}{\partial y} &= \left(2\sin(\sigma)\cosh^2(\rho/2)\right)\frac{\partial u}{\partial \rho} + \left(\frac{\cos(\sigma)}{\tanh(\rho/2)}\right)\frac{\partial u}{\partial \sigma}.\end{aligned}$$

Now, we can proceed as in Appendix A. We first find the partial derivatives of ρ and σ with respect to x and y,

$$\begin{aligned}\frac{\partial \rho}{\partial x} &= \frac{2\cosh^2(\rho/2)}{\cos(\sigma)},\\ \frac{\partial \rho}{\partial y} &= \frac{2\cosh^2(\rho/2)}{\sin(\sigma)},\\ \frac{\partial \sigma}{\partial x} &= \frac{-1}{\sin(\sigma)\tanh(\rho/2)},\\ \frac{\partial \sigma}{\partial y} &= \frac{1}{\cos(\sigma)\tanh(\rho/2)}.\end{aligned}$$

Then using the Chain Rule, we obtain the following expressions

$$\begin{aligned}\frac{\partial^2 u}{\partial x^2} &= \frac{\partial^2 u}{\partial \rho^2}(4\cosh^4(\rho/2)) + \frac{\partial u}{\partial \rho}\left(4\tanh(\rho/2)\cosh^4(\rho/2) + \frac{2\cosh^2(\rho/2)}{\tanh(\rho/2)}\right) \\ &\quad + \frac{\partial u}{\partial \sigma}\left(\frac{\sin(\sigma)}{\cos(\sigma)\tanh^2(\rho/2)} + \frac{\cos(\sigma)}{\sin(\sigma)\tanh(\rho/2)}\right) \\ &\quad - \frac{\partial^2 u}{\partial \rho \partial \sigma}\left(\frac{2\sin(\sigma)\cosh^2(\rho/2)}{\cos(\sigma)\tanh(\rho/2)}\right) - \frac{\partial^2 u}{\partial \sigma \partial \rho}\left(\frac{2\cos(\sigma)\cosh^2(\rho/2)}{\sin(\sigma)\tanh(\rho/2)}\right) \\ &\quad + \frac{\partial^2 u}{\partial \sigma^2}\left(\frac{1}{\tanh^2(\rho/2)}\right), \\ \frac{\partial^2 u}{\partial y^2} &= \frac{\partial^2 u}{\partial \rho^2}(4\cosh^4(\rho/2)) + \frac{\partial u}{\partial \rho}\left(4\tanh(\rho/2)\cosh^4(\rho/2) + \frac{2\cosh^2(\rho/2)}{\tanh(\rho/2)}\right) \\ &\quad - \frac{\partial u}{\partial \sigma}\left(\frac{\sin(\sigma)}{\cos(\sigma)\tanh^2(\rho/2)} + \frac{\cos(\sigma)}{\sin(\sigma)\tanh(\rho/2)}\right) \\ &\quad + \frac{\partial^2 u}{\partial \rho \partial \sigma}\left(\frac{2\cos(\sigma)\cosh^2(\rho/2)}{\sin(\sigma)\tanh(\rho/2)}\right) + \frac{\partial^2 u}{\partial \sigma \partial \rho}\left(\frac{2\sin(\sigma)\cosh^2(\rho/2)}{\cos(\sigma)\tanh(\rho/2)}\right) \\ &\quad + \frac{\partial^2 u}{\partial \sigma^2}\left(\frac{1}{\tanh^2(\rho/2)}\right).\end{aligned}$$

Note that when these quantities are added together, the $\partial u/\partial \sigma$ terms will cancel. Also, since we know $\frac{\partial^2 u}{\partial \rho \partial \sigma} = \frac{\partial^2 u}{\partial \sigma \partial \rho}$, these terms cancel upon adding as well. Thus we see that in polar coordinates,

$$\begin{aligned}\frac{\partial^2 u}{\partial x^2} + \frac{\partial^2 u}{\partial y^2} &= 8\cosh^4(\rho/2)\frac{\partial^2 u}{\partial \rho^2} + \left(\frac{2}{\tanh^2(\rho/2)}\right)\frac{\partial^2 u}{\partial \sigma^2} \\ &\quad + \left(\frac{4\cosh^4(\rho/2)(\tanh^2(\rho/2)+1)}{\tanh(\rho/2)}\right)\frac{\partial u}{\partial \rho}. \qquad \text{(C.3)}\end{aligned}$$

Now we must use the expression in Eq. (C.1) to determine the scale factor that we should apply to Eq. (C.3). This method follows Chavel [6, pp. 3-5]. The metric can be expressed in matrix form as

$$G = \begin{pmatrix} \frac{4}{(1-x^2-y^2)^2} & 0 \\ 0 & \frac{4}{(1-x^2-y^2)^2} \end{pmatrix},$$

where g_{jk} denotes the (j,k)-entry of the matrix, $g^{jk} = g_{jk}^{-1}$, and $\det G = g = 16/(1-x^2-y^2)^4$. The Laplacian is now given by

$$\Delta u = \left(\frac{1}{\sqrt{g}}\right) \sum_{j,k} \partial_j \left(g^{jk}(\sqrt{g})\partial_k u\right). \tag{C.4}$$

Notice that for $j \neq k$, the summand in Eq. (C.4) is zero since $g_{jk} = g^{jk} = 0$. If $j = k$, then $g_{jk} = 4/(1-x^2-y^2)^2$ and so $g^{jk} = (1-x^2-y^2)^2/4$. Also, $\sqrt{g} = \sqrt{16/(1-x^2-y^2)^4} = 4/(1-x^2-y^2)^2$ so that $g^{jk}\sqrt{g} = 1$. Thus Eq. (C.4) becomes

$$\Delta u = \left(\frac{(1-x^2-y^2)^2}{4}\right)\left(\frac{\partial^2 u}{\partial x^2} + \frac{\partial^2 u}{\partial y^2}\right). \tag{C.5}$$

Next, we must convert the term $(1-x^2-y^2)^2$. Using the substitutions in Eq. (C.2), we have

$$\begin{aligned}(1-x^2-y^2)^2 &= (1-\tanh^2(\rho/2)\cos^2(\sigma) - \tanh^2(\rho/2)\sin^2(\sigma))^2 \\ &= (1-\tanh^2(\rho/2)(\cos^2(\sigma)+\sin^2(\sigma)))^2 \\ &= (1-\tanh^2(\rho/2))^2 = \frac{1}{\cosh^4(\rho/2)}.\end{aligned} \tag{C.6}$$

Therefore, combining Eqs. (C.5) and Eq. (C.6), we have

$$\Delta u = \frac{1}{4\cosh^4(\rho/2)}\left(\frac{\partial^2 u}{\partial x^2} + \frac{\partial^2 u}{\partial y^2}\right) \tag{C.7}$$

Lastly, plugging Eq. (C.3) into Eq. (C.7), we have that the expression for the Laplacian in the Poincaré Disk is

$$\Delta u = 2\frac{\partial^2 u}{\partial \rho^2} + \left(\frac{(\tanh^2(\rho/2)+1)}{\tanh(\rho/2)}\right)\frac{\partial u}{\partial \rho} + \left(\frac{1}{2\sinh^2(\rho/2)\cosh^2(\rho/2)}\right)\frac{\partial^2 u}{\partial \sigma^2}.$$

We would like the expression in terms of functions of ρ instead of $\rho/2$. Using the relations [11, p. 490],

$$\sinh(\rho) = 2\sinh\left(\frac{\rho}{2}\right)\cosh\left(\frac{\rho}{2}\right),$$
$$\tanh\left(\frac{\rho}{2}\right) = \frac{\sinh(\rho)}{\cosh(\rho)+1},$$
$$\tanh^2\left(\frac{\rho}{2}\right) = \frac{\cosh(\rho)-1}{\cosh(\rho)+1},$$

we can obtain the following expression for the hyperbolic Laplacian,

$$\Delta u = 2\frac{\partial^2 u}{\partial \rho^2} + 2\left(\frac{\cosh(\rho)}{\sinh(\rho)}\right)\frac{\partial u}{\partial \rho} + 2\left(\frac{1}{\sinh^2(\rho)}\right)\frac{\partial^2 u}{\partial \sigma^2}. \tag{C.8}$$

D Separation of Variables for the Hyperbolic Polar Laplacian

We know the expression for the Laplacian in hyperbolic polar coordinates, Eq. (C.8). We wish to solve the equation $\Delta F + \lambda F = 0$. Now assume that $F(\rho, \sigma)$ can be separated into two functions that are each dependent on only one variable, so that $F(\rho,\sigma) \doteq T(\rho)G(\sigma)$. Applying Δ to F, we see that

$$\begin{aligned}
\Delta F &= \Delta T(\rho)G(\sigma) \\
&= 2\frac{\partial^2}{\partial \rho^2}\left(T(\rho)G(\sigma)\right) + 2\left(\frac{\cosh(\rho)}{\sinh(\rho)}\right)\frac{\partial}{\partial \rho}\left(T(\rho)G(\sigma)\right) + 2\left(\frac{1}{\sinh^2(\rho)}\right)\frac{\partial^2}{\partial \sigma^2}\left(T(\rho)G(\sigma)\right) \\
&= 2T''(\rho)G(\sigma) + 2\left(\frac{\cosh(\rho)}{\sinh(\rho)}\right)T'(\rho)G(\sigma) + 2\left(\frac{1}{\sinh^2(\rho)}\right)T(\rho)G''(\sigma),
\end{aligned}$$

where prime notation denotes differentiation with respect to the variable the in terms of which the function is given. Then

$$\Delta F + \lambda F = 2T''(\rho)G(\sigma) + 2\left(\frac{\cosh(\rho)}{\sinh(\rho)}\right)T'(\rho)G(\sigma)$$
$$+ 2\left(\frac{1}{\sinh^2(\rho)}\right)T(\rho)G''(\sigma) + \lambda T(\rho)G(\sigma) = 0.$$

Grouping terms, we have that

$$G(\sigma)\left(2T''(\rho) + 2\left(\frac{\cosh(\rho)}{\sinh(\rho)}\right)T'(\rho) + \lambda T(\rho)\right)$$
$$+2\left(\frac{1}{\sinh^2(\rho)}\right)T(\rho)G''(\sigma) = 0.$$

Then putting all terms involving T on the left and all terms involving G on the right, we have

$$\frac{\sinh^2(\rho)T''(\rho) + \cosh(\rho)\sinh(\rho)T'(\rho) + (\lambda/2)\sinh^2(\rho)T(\rho)}{T(\rho)} = -\frac{G''(\sigma)}{G(\sigma)}.$$

Since λ is an unknown, we can simply let $\lambda/2 = \lambda$. Additionally, since the left side is only dependent on ρ and the right side only dependent on σ, they must both equal a constant, which we label μ^2. Setting each side equal to μ^2 and rearranging gives the following set of equations,

$$G''(\sigma) + \mu^2 G(\sigma) = 0, \qquad \text{(D.1)}$$

$$T''(\rho) + \left(\frac{\cosh(\rho)}{\sinh(\rho)}\right)T'(\rho) + \left(\lambda - \frac{\mu^2}{\sinh^2(\rho)}\right)T(\rho) = 0. \qquad \text{(D.2)}$$

Now we can solve each of these independently. We see that Eq. (D.1) is exactly the same as Eq. (B.4) with μ in place of k. Hence the values of μ are the same as the values of k, namely, $\mu = 0, 1, 2, 3, \cdots$ and so we find solutions of Eq. (D.2) for each value of μ^2. We must do a little more work before we can recognize

Eq. (D.2). We make the change of variables $x = \cosh(\rho)$ and $T(\rho) = P(x)$. Using the Chain Rule, we have that

$$\begin{aligned}
\frac{\partial T}{\partial \rho} &= \frac{\partial P}{\partial x}\frac{\partial x}{\partial \rho} = \frac{\partial P}{\partial x}\sinh(\rho), \\
\frac{\partial^2 T}{\partial \rho^2} &= \frac{\partial}{\partial \rho}\left(\frac{\partial T}{\partial \rho}\right) = \frac{\partial}{\partial \rho}\left(\frac{\partial P}{\partial x}\sinh(\rho)\right) \\
&= \frac{\partial P}{\partial x}\cosh(\rho) + \sinh(\rho)\left(\frac{\partial^2 P}{\partial^2 x}\right)\left(\frac{\partial x}{\partial \rho}\right) \\
&= \frac{\partial P}{\partial x}\cosh(\rho) + \frac{\partial^2 P}{\partial^2 x}\sinh^2(\rho).
\end{aligned}$$

Substituting these derivatives and $x = \cosh(\rho)$ into Eq. (D.2), we have

$$\begin{aligned}
&\sinh^2(\rho)P''(x) + \left(\frac{\cosh(\rho)}{\sinh(\rho)}\sinh(\rho) + \cosh(\rho)\right)P'(x) + \left(\lambda - \frac{\mu^2}{\sinh^2(\rho)}\right)P(x) \\
&= (x^2-1)P''(x) + 2xP'(x) + \left(\lambda - \frac{\mu^2}{(x^2-1)}\right)P(x) = 0,
\end{aligned}$$

and multiplying by -1 gives us

$$(1-x^2)P''(x) - 2xP'(x) + \left(-\lambda - \frac{\mu^2}{(1-x^2)}\right)P(x) = 0. \tag{D.3}$$

Finally, if we let

$$\nu = -\frac{1}{2} \pm \left(\sqrt{\frac{1}{4} - \lambda}\right),$$

then $\nu(\nu+1) = -\lambda$ for either choice of sign, so Eq. (D.3) becomes

$$(1-x^2)P''(x) - 2xP'(x) + \left(\nu(\nu+1) - \frac{\mu^2}{(1-x^2)}\right)P(x) = 0. \tag{D.4}$$

Equation (D.4) is known as an Associated Legendre equation and its solution is the Associated Legendre function of degree ν and order μ, denoted P_ν^μ. Associated Legendre functions can be defined explicitly but we omit the definition since it is quite complex and we do not require it. They have been well studied and are similar in nature to Bessel functions. However, they are generally more complex than Bessel functions and have zeroes that are more difficult to find. Theoretically, we treat the two types of functions similarly in terms of finding eigenvalues. In particular, the eigenvalues of Eq. (D.4) and hence of Eq. (D.2) are zeros of $P^{\mu}_{\nu}(x) = P^{\mu}_{\nu}(\cosh(\rho))$. As in Appendix B, the eigenvalues of F are simply the eigenvalues of T and hence the eigenvalues of F are zeros of $P^{\mu}_{\nu}(\cosh(\rho))$.

E Mathematica Code to Numerically Investigate the Fundamental Gap

Provided in this section is the Mathematica code described in Section 9 used to test our conjectured upper bound for the fundamental gap. Some formatting has been added for this presentation.

```
n = 1000;
Array[Gaps, n, 1];
Array[InRads, n, 1];
Array[OutRads, n, 1];
Array[Counter, n, 1];
counter = 0;
For[i = 1, i ≤ n, i++,
alpha = RandomReal[0, Pi/2];
beta = RandomReal[0, Pi/2];
gamma = RandomReal[0, Pi/2];
sinha = Abs[Sqrt[((1/2)*(((Cos[beta]*Cos[gamma] +
        Cos[alpha])/(Sin[beta]*Sin[gamma])) - 1))]];
sinhb = Abs[Sqrt[((1/2)*(((Cos[alpha]*Cos[gamma] +
```

```
        Cos[beta])/(Sin[alpha]*Sin[gamma])) - 1))]];
sinhc = Abs[Sqrt[((1/2)*(((Cos[alpha]*Cos[beta] +
         Cos[gamma])/(Sin[alpha]*Sin[beta])) - 1))]];
sigma = (alpha + beta + gamma)*(1/2);
test1 = If[Pi < alpha + beta + gamma, 0, 1];
test2 = If[sinha < (sinhb + sinhc) && sinhb < (sinha + sinhc)
        && sinhc < (sinha + sinhb), 1, 0];
inradius = N[ArcTanh[Sqrt[(((Power[Cos[alpha],2] + Power[Cos[beta],2]
    + Power[Cos[gamma],2] + 2*Cos[alpha]*Cos[beta]*Cos[gamma] - 1)
        /(2*(1 + Cos[alpha])*(1 + Cos[beta])*(1 + Cos[gamma])))]]];
outradius = N[ArcTanh[Sqrt[(Cos[sigma]/
        (Cos[sigma - alpha]*Cos[sigma - beta]*Cos[sigma - gamma]))]]];
Elambda1in = Power[2.40483/inradius,2];
Elambda2in = Power[3.83171/inradius,2];
gamma = Exp[1 + Sqrt[4*Power[outradius,2]]];
Ratio = Elambda2in/Elambda1in;
Bound = (1/4) + Power[2*Pi/inradius,2];
lambda1outbound = (1/gamma)*((1/(4*Power[outradius,2])
        *Power[Log[gamma],2] - 1);
TriangleGapBound = Ratio*Bound - lambda1outbound;
test3 = If[Im[TriangleGapBound] == 0, 1, 0];
testsum = (test1 + test2 + test3)/3;
If[testsum == 1,
Gaps[i, 1] = TriangleGapBound;
InRads[i, 1] = inradius;
OutRads[i, 1] = outradius;
Counter[i, 1] = 1, Counter[i, 1] = 0] ;
```

```
counter = counter + Counter[i, 1]; ] counter
For[i = 1, i <= counter, i++,
Write["NewGaps.xls", Gaps[i, 1 ]];
Write["NewInRads.xls", InRads[i, 1]];
Write["NewOutRads.xls", OutRads[i, 1]];]
```